Bioresource Technology 336 (2021) 125329

Contents lists available at ScienceDirect

Bioresource Technology

journal homepage: www.elsevier.com/locate/biortech

Comprehensive evaluation of different strategies to recover methanogenic performance in ammonia-stressed reactors

Miao Yan [a], Xinyu Zhu [b], Laura Treu [c], Giulia Ravenni [d], Stefano Campanaro [c], Estelle Maria Goonesekera [a], Rosa Ferrigno [a], Carsten S. Jacobsen [e], Athanasios Zervas [e], Irini Angelidaki [b,1], Ioannis A. Fotidis [f,g,a,1,*]

[a] Department of Environmental Engineering, Technical University of Denmark, Building 115, Kgs. Lyngby DK-2800, Denmark
[b] Department of Chemical and Biochemical Engineering, Technical University of Denmark, Building 227, Kgs. Lyngby DK-2800, Denmark
[c] Department of Biology, University of Padova, Via U. Bassi 58/b, Padova 35121, Italy
[d] Department of Chemical and Biochemical Engineering, Technical University of Denmark, Building 313, Roskilde 4000, Denmark
[e] Department of Environmental Science, Aarhus University, Frederiksborgvej 399, Roskilde DK-4000, Denmark
[f] Faculty of Engineering and Natural Sciences, Tampere University, Tampere, Finland
[g] School of Civil Engineering Southeast University Nanjing, 210096, China

HIGHLIGHTS

- Bioaugmentation with ready-to-use inocula was demonstrated for the first time.
- Bioaugmentation with gel-preserved consortium raised the R_{max} by 77%.
- Wood biochar raised the R_{max} by 35%.
- Straw biochar induced selective raise of *M. thermophila* under ammonia stress.
- Woodchip biochar possibly contributed to interspecies Direct Electron Transfer.

GRAPHICAL ABSTRACT

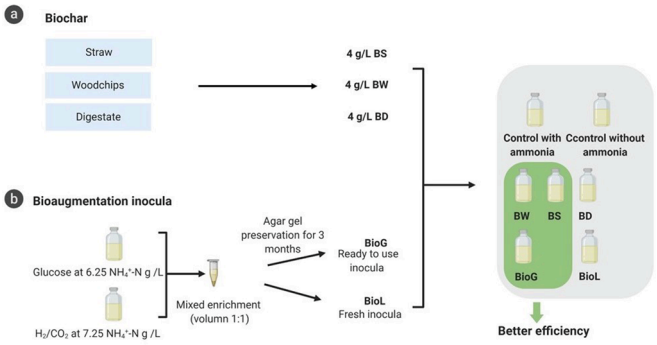

ARTICLE INFO

Keywords:
Bioaugmentation
Biochar
Ammonia Inhibition
Anaerobic Digestion
Selective Enrichment

ABSTRACT

In this study, strategies for recovery of ammonia-stressed AD reactors were attempted, by addition of preserved bioaugmentation consortium in gel (BioG), fresh consortium in liquid medium (BioL), woodchip biochar (BW), and straw biochar (BS). In comparison to control group with ammonia, effective treatments, i.e., BioG, BioL, BW and BS raised the maximum methane production rate by 77%, 23%, 35%, and 24%, respectively. BW possibly acted as interspecies electrical conduits for Direct Electron Transfer based on conductivity and SEM analysis. BioG facilitated slow release of bioaugmentation inocula from gel into the AD system, which protected them from a direct environmental shock. According to microbial analysis, both BioG, BioL and BW resulted in increased relative abundance of *Methanothermobacter thermautotrophicus*; and BS induced selective raise of *Methanosarcina thermophila*. The increase of methanogens via these strategies led to the faster recovery of the AD process.

* Corresponding author.
E-mail address: ioannis.fotidis@tuni.fi (I.A. Fotidis).
[1] These authors contributed equally.

https://doi.org/10.1016/j.biortech.2021.125329
Received 21 April 2021; Received in revised form 20 May 2021; Accepted 21 May 2021
Available online 25 May 2021

1. Introduction

Anaerobic digestion (AD) involves intricate microbial networks dedicated to the degradation of organic matter into methane and represents a promising energy-recovery based organic waste treatment technology (Campanaro et al., 2020; Cao and Pawłowski, 2012). Nevertheless, N-rich organic waste in full-scale AD treatments may decrease the process efficiency (Tian et al., 2018). In particular, free ammonia can inhibit microbial activity by: 1) changing intracellular pH, 2) inactivating of enzymes related to methanogenesis, 3) severe osmotic stress (Capson-Tojo et al., 2020; Frank et al., 2016). It is important to underline that methanogens are more vulnerable to ammonia toxicity compared to bacteria involved in hydrolysis, acidogenesis and acetogenesis. The inhibited methanogenic activity would cause low methane production yields, and accumulation of volatile fatty acids (VFAs) (Treu et al., 2019; Yan et al., 2019). Therefore, effective strategies to provide methanogens more resistant to high ammonia concentrations, or able to stimulate their growth are urgent to recover energy from N-rich organic wastes.

Recent researches have reported successful remediation of ammonia inhibition by adding ammonia-tolerant methanogens directly into the digesters (Fotidis et al., 2013; Tian et al., 2019a; Yan et al., 2020c). However, in order to be able to timely react and implement effective full-scale bioaugmentation, it would require availability of ready to use bioaugmentation inocula. For this reason, the ready-to-use ammonia tolerant methanogenic inocula is a promising tool to reduce the preparation time and to achieve efficient bioaugmentation Therefore, evaluating for the first time these long-term preserved inocula as bioaugmentation inocula to alleviate ammonia inhibition was performed in this study.

Other approaches to counteract ammonia stress have been developed for AD systems, such as ammonia removal by struvite precipitation, ammonia-absorbent (zeolite and active carbon, etc.), and ammonia stripping (Capson-Tojo et al., 2020). Unfortunately, their commercial applications in biogas plants are limited due to high energy consumption, addition of chemicals, increased complexity of operation, resulting in negative economic and environmental impact (Qiu et al., 2019). Biochar is the solid product of biomass thermal decomposition under oxygen-limited conditions, hence it can be obtained via pyrolysis or gasification of the feedstock (Basaglia et al., 2021; Schmidt et al., 2013). It has been recently proposed as a sustainable and effective metal-free catalyst in the mineralisation of organic matter due to its characteristics (Hu et al., 2020; Tian et al., 2020). First, the porous structure and the presence of surface functional groups (e.g., oxygen groups, sulphur groups, and acidic groups) enable its capability of ammonia adsorption (Qiu et al., 2019). Second, the alkalinity of biochar enhances the pH buffering capacity of the AD systems (Wei et al., 2020). Third, the large specific surface area provides a favourable environment for microbes retention and growth (Qiu et al., 2019). Fourth, electrochemical carbocatalysis (reactive-active moieties or highly reactive oxygen species) of biochar promotes electron transfer for organic matter degradation (Wan et al., 2020). Additionally, the incorporation of biochar into digestate can improve its quality as a soil amendment and fertilizer compared to non-biological approaches (Masebinu et al., 2019). However, the properties of biochar can vary significantly depending on the feedstock and the operating conditions of the thermochemical process (Qiu et al., 2019). Previous research proposed that biochar derived from lignin-rich biomass is more likely to have an ordered carbon structure, favourable for the formation and preservation of reactive active moieties than biochar obtained from ash-rich biomass (Wan et al., 2020). In particular, wood- or straw-derived biochars have shown eminent preponderance to degrade organic waste through directly interacting with chemicals by inherent reactive active moieties (Sun et al., 2019; Wan et al., 2020). Biochar derived from digestate is attracting researcher attention to improve AD systems as well (Ambaye et al., 2020). These studies focused on recovering AD from ammonia inhibition using different methods, such as different types of biochar and bioaugmentation, but either only one type of biochar (Ambaye et al., 2020) or only bioaugmentation was investigated in most of the cases (Tian et al., 2019a) without comparison with other methods. A holistic comparison of different recovery methods is still lacking, particularly under the same operational conditions.

This study aims to assess the effect of different AD process recovery strategies (i.e. bioaugmentation with gel preserved and liquid inocula, and addition of biochars derived from woodchip, straw and digestate) in anaerobic digesters suffering from ammonia toxicity. The efficiency to recover under-performing AD systems was assessed by monitoring two key parameters: changes in the methane production and VFAs concentrations. Furthermore, measurements of the total ammonia nitrogen (TAN) adsorption and the electrical conductivity, as well as the scanning electron microscopy (SEM) for determine the microbial's distributions and compositions were employed to explain the performance of each applied strategy.

2. Material and methods

2.1. Materials

2.1.1. Digestate

The digestate was collected from a thermophilic biogas plant (Lemvig Biogas A.m.b.A. Pillevej 12). Total solids (TS) and volatile solids (VS) of the digestate were determined according to the standard methods (APHA, 2005), with the results of 33 ± 1.2 g/L and 14.4 ± 0.9 g/L, respectively.

2.1.2. Bioaugmentation inocula

Two ammonia tolerant microbial consortia were cultivated in thermophilic batch reactors with a total volume of 1.5 L, using glucose at 6.25 NH_4^+-N g/L and H_2/CO_2 at 7.25 NH_4^+-N g/L as carbon and energy sources in basal anaerobic (BA) medium separately. The final cultures were harvested when the volatile suspended solids (VSS) concentration of 78 and 39 mg/L, were reached respectively. According to microbial analysis, the methanogenic communities fed with glucose and H_2/CO_2 were dominated by *Methanothermobacter* sp. (Yan et al., 2020d) and *Methanothermobacter thermautotrophicus* sp., respectively. The two enriched consortia were mixed based on the volume ratio of 1:1 (v/v), then upconcentrated through centrifugation at 4500 rpm for 10 min under N_2 gas headspace (Tian et al., 2019b). Three levels of culture concentrations (i.e., 58.5, 117 and 176 mg VSS/L) were tested. Finally, 10 mL microbial enrichments were preserved in 4 mL agar gel for 90 days, as previously described (Yan et al., 2020a), providing a ready-to-use methanogenic enrichment culture.

2.1.3. Biochar preparation

Three types of commonly used biochars were applied in this work. Biochars derived from straw and spruce woodchip were obtained from pilot-scale gasification plants operated at Technical University of Denmark. Straw biochar was the solid residue of Low-Temperature Fluidized Bed gasification, with a maximum process temperature of 750°C. Woodchip biochar was generated by Two-Stage gasification, a process which reaches a maximum temperature of about 1100°C. Further details about these materials and the gasification technologies can be found in previous publication (Hansen et al., 2015). Biochar from digestate fibers was obtained via batch pyrolysis at 600°C (10°C/min heating rate, 1 h hold time) (Yang et al., 2016). All the biochars were ground and sieved to achieve particles in the size range of 0.5–1 mm, then dried at 105°C for 24 h before use. The specific surface area of biochar samples was quantified by Brunauer-Emmett-Teller (BET) analysis through N_2 adsorption at 77 K (NovaTouch, Quantachrome Instruments, USA). The ash content was measured by complete oxidation of the samples at 550°C for 2 h, while the pH was measured by mixing the samples with deionised water at the ratio of 1:10 (w/w). The

obtained properties of the biochars are listed in Table 1.

2.1.4. Experimental set-up

Based on the preliminary experiments, 4 g/L biochar with 117 mg VSS/L enriched consortium in gel, and 176 mg/L (VSS) enriched consortium in liquid medium were selected as the optimum dosage, considering the alleviation effect and the application cost. The experiments were performed in batch reactors fed with Avicel (Avicel® PH-101, Sigma Aldrich), each with a 50 and 238 mL working and total volume, respectively (Fig. 1). In order to pinpoint the appropriate strategy for alleviating ammonia stress, the batch reactors were divided in eight groups with different conditions, as listed in Table 2. Each group included three reactors, so that all conditions were tested in triplicate. After being flushed with N_2, all the bottles were sealed and placed in an incubator at 55°C, with daily hand agitation until the end of the experiment. The final solution pH was fixed at 8.0 ± 0.1 using 4 mol/L hydrochloric acid or 4 mol/L sodium hydroxide. Gas and liquid samples were periodically collected until methane production stopped.

2.2. Analyses

2.2.1. Chemical analyses

Methane and volatile fatty acids (VFA) concentrations were measured using methods based on a previous study (Yan et al., 2020c). pH, TS, VS, VSS, and TAN were determined according to the standard methods for the examination of water and wastewater (APHA, 2005).

2.2.2. Physical analyses

The microbial distribution in each group was visualized by SEM using an FEI Helios EBS3 dual-beam electron microscope. The conductivity of the sludge samples from each group was assessed with a three-probe electrical conductance measurement using two gold electrodes. Conductivity calculation was carried out using Ivium software (IVIUM, The Netherlands). The samples preparation for SEM and the conductivity measurements were performed following the same procedures as in Wang et al. (2018).

2.2.3. Microbial analysis

The samples for DNA extraction were collected from each group (Table 2) at the end of the incubation. After a cleaning step with Phenol: Chloroform: Isoamyl Alcohol (25: 24: 1), the DNA extraction was performed using DNeasy PowerSoil® (QIAGEN GmbH, Hilden, Germany). PCR amplification was conducted on the V4 region of the 16S rRNA gene using universal primers 515F/806R and high throughput sequencing was run through Illumina MiSeq platform at the Department of Environmental Science, Aarhus University. Raw reads were deposited in Sequence Read Archive (SRA) database with the name of SUB9042235.

The raw data were processed using CLC Workbench software (20.0.4) with the microbial genomics module plugin as previously described (Treu et al., 2018). Briefly, operational taxonomic unit (OTU) clustering was defined at 97% sequence similarity. The relative abundances of dominant OTUs were visualised by Multi Experiment Viewer software (MeV 4.9.0). Beta diversity (Principal Component Analysis (PCA)) was calculated and plotted by STAMP software. Statistical analyses of microbial networks were performed in R software. Specifically, Spearman's correlation coefficient >0.6 and statistically significant (p-value) <0.05 were set to obtain strong correlations among taxon and intermediates (Schober et al., 2018). The networks were then visualised using Gephi (Bastian et al., 2009).

Table 1
Properties of biochar used in the experiments.

Biochar	Particle size (μm)	Ash content (wt%)	BET surface area (m^2/g)	pH	TAN removal (mg/g)	
BS	500–1000	55.20%	12.00	11.24	6.65	0
BW		9.40%	766.00	10.08	41.94	–
BD		79.80%	5.50	10.15	15.47	0

2.2.4. Maximum methane production

The maximum methane potential of the Avicel (i.e. 0.415 CH_4 mL/g VS) was calculated according to Eq. (1) where complete conversion of organic matter to CH_4 and CO_2 was assumed.

$$CnHaOb + \left(n - \frac{a}{4} - \frac{b}{2}\right) H2O \rightarrow \left(\frac{n}{2} + \frac{a}{8} - \frac{b}{4}\right) CH4 + \left(\frac{n}{2} - \frac{a}{8} + \frac{b}{4}\right) CO2 \quad (1)$$

2.2.5. Methane production modelling using the modified Gompertz model

The modified Gompertz model (by Excel) was employed to quantitatively estimate all experiments (Eq. (2)), based on P maximum methane potential (mL CH_4/g VS), methane production M(t) (mL CH_4/g VS) at time t, λ lag phase (d), and R_{max} the maximum methane production rate (mL CH_4/g VS/d).

$$M(t) = P^{*}exp\left(- exp\left(\frac{R\ max}{P}{*}e(\lambda - t) + 1\right)\right) \quad (2)$$

TAN removal efficiency was obtained using Eq. (3) q_t (mg/g), where Ci and Cf (mg/L) are the initial and final NH_4^+-N concentration in solution, respectively; qt (mg/g) was the adsorbed amount of NH_4^+-N, V (L) was the volume of digestate, and M (g) the mass of biochar.

$$qt = \frac{Ci - Cf}{M} {*} V \quad (3)$$

3. Results and discussion

3.1. Effect of ammonia alleviation strategies on methane production

The best performing ammonia alleviation strategies were BioG, BW, and BS, followed by BioL, while the BD strategy led to a slightly adverse effect on methane production with decreased R_{max} (Fig. 2a and b). Specifically, CWOA had a R_{max} of 19.4 mL CH_4/g VS·d (Fig. 2b). As expected, higher ammonia in CWA decreased R_{max} to 13.9 mL CH_4/g VS·d.

Specifically, BW, BS, BioL, and BioG increased R_{max} by 35%, 23%, 23% and 77%, respectively but BD decreased R_{max} by 18% (Fig. 2b). In BioG, the highest R_{max} along with the shortest incubation time suggested a prominent advantage to remedy ammonia-stressed AD with this method. Furthermore, BS and BW showed faster in-situ recovery of microbial activities than BioL and BioG. As supported by previous researches, the addition of wood-derived biochar in AD facilitated the methanogenic adaptation to environmental stress (Lü et al., 2019; Luo et al., 2015).

The lowest R_{max} in BD indicated that methanogenic activity was inhibited. A possible explanation is that toxic elements present in the digestate were highly condensed and immobilised into biochar during the pyrolysis process (Xie et al., 2020). The leaching and dissolution of chemical elements (e.g. Ca and Mg) from BD could have also contributed in the toxic effect as e.g. 5 g L-1 have inhibitory effect on AD process according to previous studies (Ahn et al., 2006; Romero-Güiza et al., 2016). Interestingly, an increased methane production was observed upon the addition of sewage sludge biochar in another study (Ambaye et al., 2020), but still was no able to prevent mild ammonia inhibition at just 2.1 g NH_4^+-N/L (Mumme et al., 2014). Hence, the efficiency of BD seemed to depend on the feedstock composition and was generally unfavourable in terms of ammonia stress remediation. Therefore, BioG provided the highest R_{max} to all examined remediation strategies, BW and BS showed advantages in reducing the incubation time and λ when compared with bioaugmentation strategies.

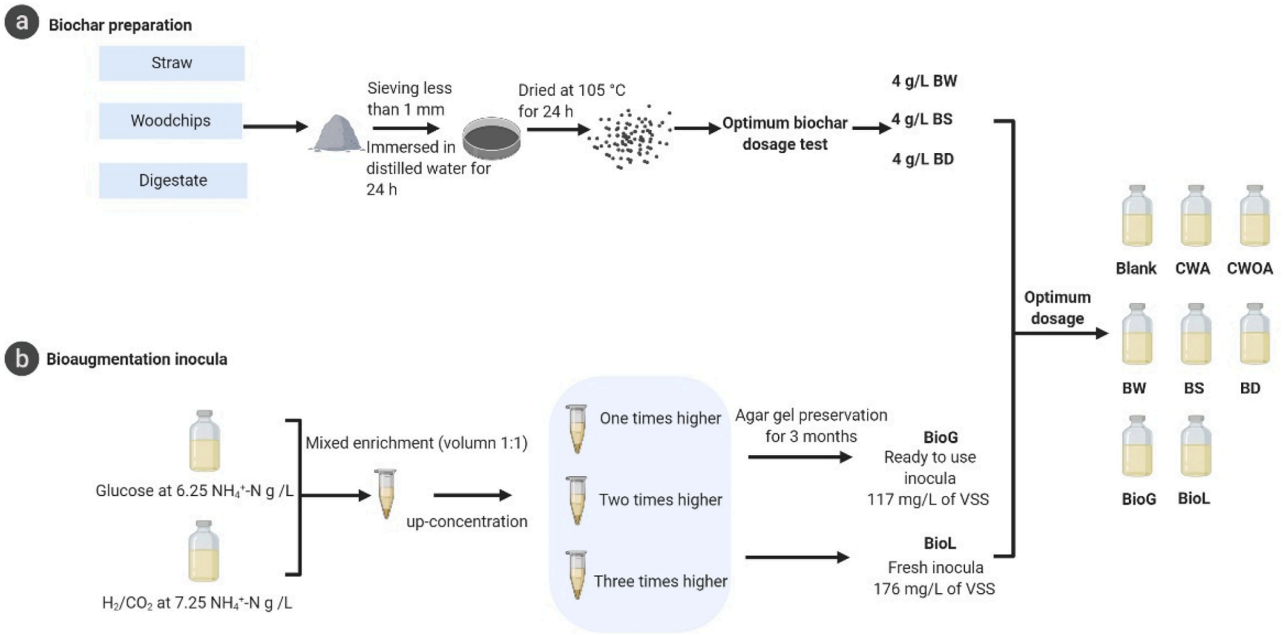

Fig. 1. Diagram of the multiple strategies developed to alleviate ammonia stress.

Table 2
The characteristic of each experimental group.

Strategy	Composition of each group
Blank	10 mL digestate + 40 mL water
Control group without ammonia (CWOA)	10 mL digestate + 2.4 g/L Avicel + 40 mL water
Control group with ammonia (CWA)	10 mL digestate + 2.4 g/L Avicel + 40 mL water + 4 g NH_4^+-N/L (Ammonium chloride)
Bioaugmentation using gel preserved consortium (BioG)	10 mL digestate + 2.4 g/L Avicel + 26 mL water + 4 g NH_4^+-N/L + 10 mL of consortium entrapped in 4 mL of agar gel (117 mg VSS/L)
Bioaugmentation using liquid fresh consortium (BioL)	10 mL digestate + 2.4 g/L Avicel + 30 mL water + 4 g NH_4^+-N/L + 10 mL of consortium (176 mg VSS/L)
Straw biochar (BS)	10 mL digestate + 2.4 g/L Avicel + 40 mL water + 4 g NH_4^+-N/L + 4 g/L straw biochar
Woodchip biochar (BW)	10 mL digestate + 2.4 g/L Avicel + 40 mL water + 4 g NH_4^+-N/L + 4 g/L woodchip biochar
Digestate biochar (BD)	10 mL digestate + 2.4 g/L Avicel + 40 mL water + 4 g NH_4^+-N/L + 4 g/L digestate biochar

3.2. Acetate profile

The concentration of acetate is an indicator of the balance between acetogenesis and methanogenesis. As expected, BW and BioG triggered a faster acetate metabolism. Surprisingly, higher acetate levels accumulated in BS during the last 30 days of the AD process, compared to the control group with ammonia (CWA). Specifically, during the first 8 days, the acetate concentration of the different batches increased and reached the peak of 1870 mg HAc/L (BioG), 1714 mg HAc/L (BW), 1468 mg HAc/L (BioL), and 1391 mg HAc/L (BS), all higher than CWA (1143 mg HAc/L). The differences between these treatments and CWA indicated that all strategies except BD accelerated the acetogenesis process in the early stage (Fig. 2a and c). From days 9 to 22, the rate of acetate consumption became faster than acetate production. On day 22, the acetate concentration of 429 mg HAc/L in CWA suggested an imbalance between acetate production and consumption rate due to ammonia inhibition (being significantly higher than CWOA ($p < 0.01$)). Meanwhile, the lower acetate levels in BW (29 mg HAc/L), BioL (81 mg HAc/L), and BioG (133 mg HAc/L) proved their ability to alleviate the acetate accumulation due to ammonia inhibition (Fig. 2c). The slower acetate degradation process in BS and BD was possibly due to the high ash content of the biochars (Table 1). In fact, a recent research found that increased ash content might favour the dissolution of biochar causing cation toxicity (Masebinu et al., 2019). Besides, biochar microspores being blocked by ash might limit the microbial proliferation, and the efficiency in regulating electron transfer between substrate and microbes (Zhang et al., 2019).

3.3. How each strategy affects AD performance

3.3.1. Gel preserved versus liquid fresh consortia bioaugmentation

The addition of methanogenic culture in BioG and BioL led to a faster acetate metabolism and enhanced R_{max}, suggesting that the inhibiting effect of ammonia on intermediates (e.g. acetate) conversion was reduced. Furthermore, the BioG showed higher R_{max} compared to BioL during the catabolism of Avicel. The possible reason was the slow release of gel into the AD system, which enabled the microbes to gradually expose to the new environment and thus shielded them from a direct shock. This hypothesis is supported by previous studies (Yan et al., 2020b). Bioaugmentation with ready-to-use inocula was developed and demonstrated for the first time in this work and could fully recover ammonia-inhibited AD processes.

3.3.2. Total ammonia nitrogen removal

The ability of biochar to adsorb ammonia in-situ should contribute towards reducing ammonia stress on microorganisms. According to the TAN analysis (Table 1), woodchip biochar showed the highest adsorption of 41.94 mg NH_4^+-N/g biochar from the liquid phase, which should be attributed to the large BET surface area (766 m^2/g). By contrast, straw and digestate biochar exhibited lower TAN adsorption (6.7 and 15.5 mg NH_4^+-N/g biochar, respectively), probably because of their lower surface area compared to woodchip biochar (Table 1). The differences in TAN adsorption for the different biochars were well matched to their AD performance. This finding was in agreement with previous studies, highlighting that higher TAN adsorption capacity leading to better ammonia remediation (Qiu et al., 2019; Zhang et al., 2019).

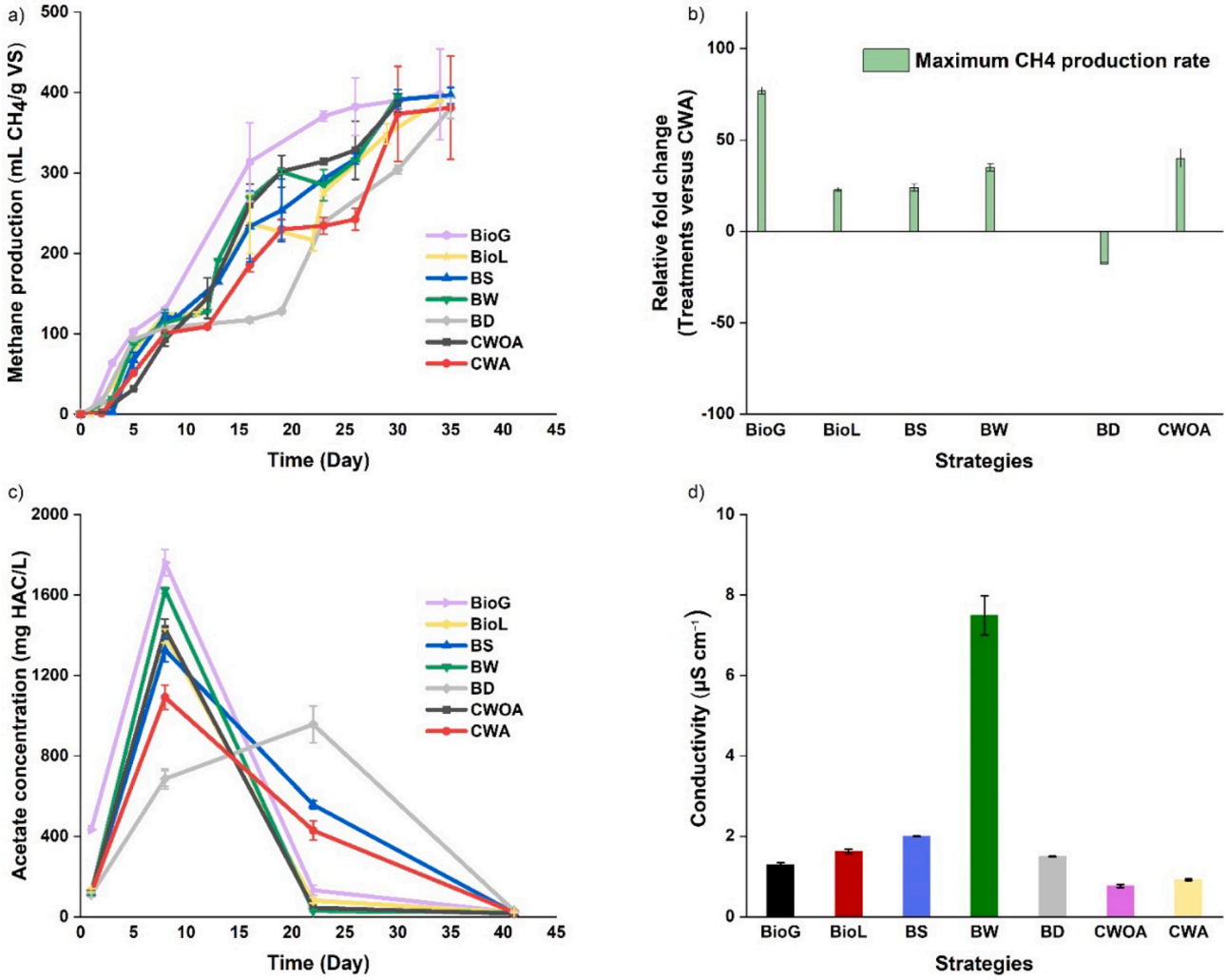

Fig. 2. Effects of different ammonia-toxicity alleviation strategies on AD process: a) methane production profile; b) lag phase and maximum methane production rate; c) acetate metabolism; d) conductivity ratio of sludge samples to 0.1 mol NaCl solution. BioG: Bioaugmentation using gel preserved consortium; BioL: Bioaugmentation using liquid fresh consortium; BS: Straw biochar; BW: Woodchip biochar; BD: Digestate biochar, CWOA: Control group without ammonia; CWA: Control group with ammonia.

3.3.3. *Sludge physiological properties*

In this study, the highest conductivity was observed in the BW with almost 8-fold higher value than the 0.1 mol NaCl solution, and followed with BS, BioL, BD, and BioG, ranging from 0.7- to 2-fold. As supported by the SEM images the microorganisms were scattered on the surface of woodchip biochar, rather than aggregated to each other for making biological electrical connections in other groups. These observations indicated that woodchip biochar possibly acted as interspecies electrical conduits for Direct Electron Transfer (DIET) thanks to its high conductivity. The establishment of DIET via woodchip biochar possibly eliminated the requirement for biological connection or proximity and promoted the electron transfer between syntrophic co-cultures e.g., *M. thermautotrophicus* sp.3, *Syntrophomonadaceae* sp.22 and *S. schinkii* sp.28 (Fig. 4b). Similarly, another study reported that the conductivity of biochar was the primary reason for the improved AD performance (Zhao et al., 2015a).

Redox-active functional groups and the polyaromatic carbon matrices present in biochar have been reported as the major elements responsible for the electron transfer (Qiu et al., 2019; Sun et al., 2018). Besides, at high pyrolysis temperature above 650°C, ordered aromatic structure developed, leading to improved direct electron transfer (Sun et al., 2018; Wan et al., 2020). Thus, the higher conductivity of woodchip biochar compared to the other biochars in this work can be explained by the higher pyrolysis temperature, together with its low ash content. Furthermore, the SEM images showed that only BW promoted microbial biofilms formation, which colonised woodchip biochar. According to previous research, biofilm facilitates microbial protection against environmental stress factors (Zhao et al., 2015b).

3.3.4. *Insights into microbial communities*

3.3.4.1. Beta diversity. The beta diversity was used to visualise the difference in community composition among groups. Clearly, the initial common microbiota was driven into forming distinct communities (Fig. 3). Specifically, the points of CWOA and BW clustered more closely compared to other treatments, suggesting similar population structures (Fig. 3). Woodchip biochar perhaps protected the microbiota from ammonia shock, as discussed in sections 3.3.1 and 3.3.2. On the other hand, straw biochar steered microbiota toward BioG and BioL groups. Results revealed that these two types of biochar and bioaugmentation strategies equally harboured the potential to optimise microbial community structure. Conversely, the under-performing biomethane process of the BD microbiome was far from the CWOA and the other productive groups.

3.3.4.2. Shift of microbial composition in response to different strategies.

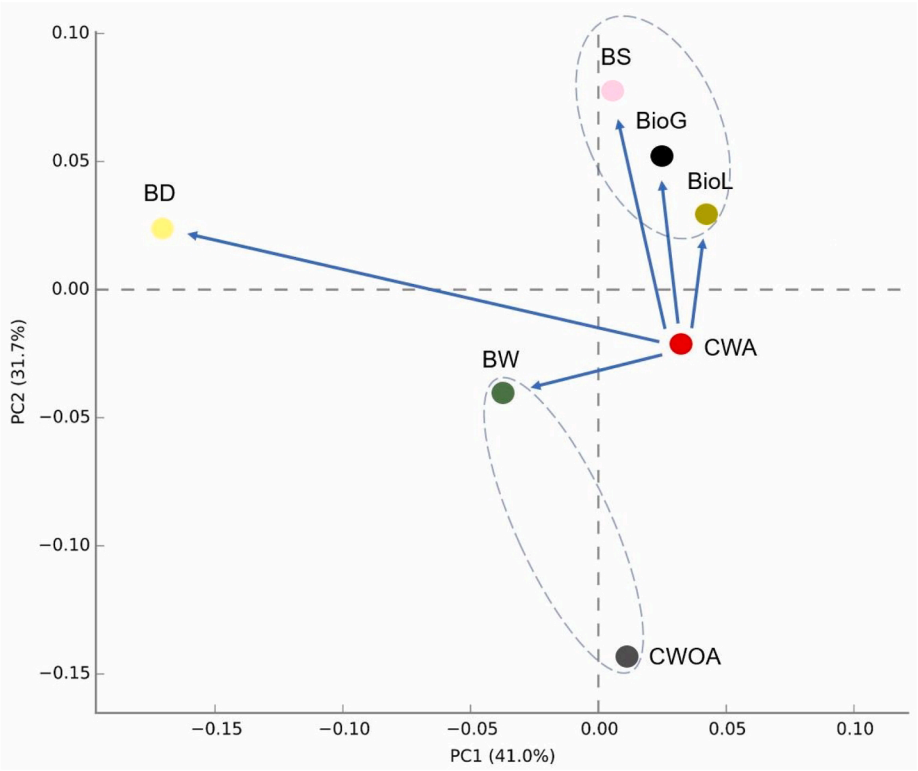

Fig. 3. Beta diversity of each group. Principal components (PC) 1 and 2 explained 41.0% and 31.7% of community variation, respectively.

The main six phyla present in seven groups were *Firmicutes* (78–86%), *Synergistetes* (1.2–3.8%), *Thermotogae* (1.0–2.7%), *Bacteroidetes* (1–2%), *Cyanobacteria* (0–0.2%) and *Euryarchaeota* (0.6–2.1%) (Fig. 4a). The results indicated that different strategies did not change microbial composition on phylum level excepting for *Euryarchaeota* (a 3-fold increase in the BioG, BS, and BW treatments), in compared to CWA.

Thus, the higher resolution into microbial community composition at species level are visualized including the top 29 OTUs (>0.1% relative abundance), selected as representatives of the whole community (Fig. 4b). The bacterial species related to the substrate hydrolysis process mainly included *Clostridiaceae* sp.14, *Halanaerobiaceae* sp.16, *Peptococcaceae* sp.18, and *SHA-98* sp.19. Their cumulative relative abundance was 30.5% (BD), 17% (CWA, BioG, BS, and BW), and followed by 8 and 11% for CWOA and BioL, respectively. The other dominant bacteria were glucose degraders, e.g., *Thermoanaerobacteraceae* sp.13. The highest relative abundance of glucose degraders was 33% (CWOA), followed by 20–27% (CWA, BioL, BW, and BD), and 15% (BioG and BS). Microbial network analysis over each group suggests *Caldicoprobacteraceae* spp.11, *Thermoanaerobacteraceae* sp.13, and *SHA-98* sp.19 were positively associated with other acetogens and methanogens, and the multiple small worlds they formed might act as a strong buffer against environmental change (Fig. 6).

Acetomicrobium mobile sp.9, *Thermoanaerobacter brockii* subsp. *finnii* sp.*8*, *Syntrophaceticus schinkii* sp.*28* and *Syntrophomonadaceae* sp.22 were assigned to well-known syntrophic microorganism capable of generating electricity and degrading fatty acids (Dyksma et al., 2020; Masebinu et al., 2019; Wang et al., 2018). For example, the significant negative correlation ($p < 0.01$) between *A. mobile* sp.9 and acetate concentration demonstrated its contribution to acetate consumption (Fig. 6). Compared to the control with ammonia (a cumulative relative abundance of 13%), the relative abundance of these taxa was higher in CWOA (14%), BW (23%) and BS (20%). These results suggest that these conductive materials (especially BW) stimulated syntrophic interactions, which agrees with previous study that syntrophism of these genera was enhanced 1.5 times due to the addition of magnetite, leading to an increased methane production (Wang et al., 2018). A well-known SAOB, i.e. *S. schinkii* sp.28 was selectively enriched by 9-fold in BW compared with CWA and showed a proportional increase with *Methanothermobacter thermautotrophicus* sp.3 (Fig. 4b). As reported by previous studies, the addition of *S. schinkii* alone, neither stimulated the growth of the syntrophic hydrogenotrophic methanogen nor improved process performance against ammonia inhibition (Westerholm et al., 2012). Furthermore, bioaugmentation with *M. thermautotrophicus* sp.3 did not induce the increase of *S. schinkii* sp.28 in BioG. These results suggest that woodchip biochar provided a favourable environment to enable simultaneous growth of *M. thermautotrophicus* sp.3 and *S. schinkii* sp.28, thus leading to faster recovery of the AD process.

Seven methanogenic OTUs within four different orders (*Methanobacteriales*, *Methanomicrobiales*, *Methanosarcinales*, and *Methanomassiliicoccus*) were found in most groups, indicating highly diverse methanogenic communities (Fig. 5). This heterogeneity could be regarded as a natural reservoir of "low active" species, which can preserve the functional diversity and the ability to take over methane production once exposed to environmental changes (Campanaro et al., 2018). Specifically, most abundant methanogens *M. thermautotrophicus* sp.3 (0.9% of relative abundance) in CWOA indicated that methane was mainly produced through the hydrogenotrophic methanogenesis. Indeed, the decrease of *M. thermautotrophicus* sp.3 to 0.5% in CWA and BD, revealed the inhibiting effect of ammonia on its growth. In contrast, its abundance increased in BioG (1.9%), BW (1.8%), and BioL (0.6%), except in BS (0.1%). It is worth mentioning that the higher relative abundance of bioaugmentation inocula i.e., *M. thermautotrophicus* sp.3, in BioG than BioL group, is likely attributed to the slow release of gel protecting microbes from a direct environmental shock. This increase was correlated to the methanogenic activity, such as increased methane production rate and reduced VFA levels. Acetoclastic methanogens were rarely detected in the above groups, and only BS harboured a distinct archaeal community dominated by *Methanosarcina thermophila* sp.6 (1.8%). According to previous research, *M. thermophila* was able to perform biphasic methane production from multiple methanogenic

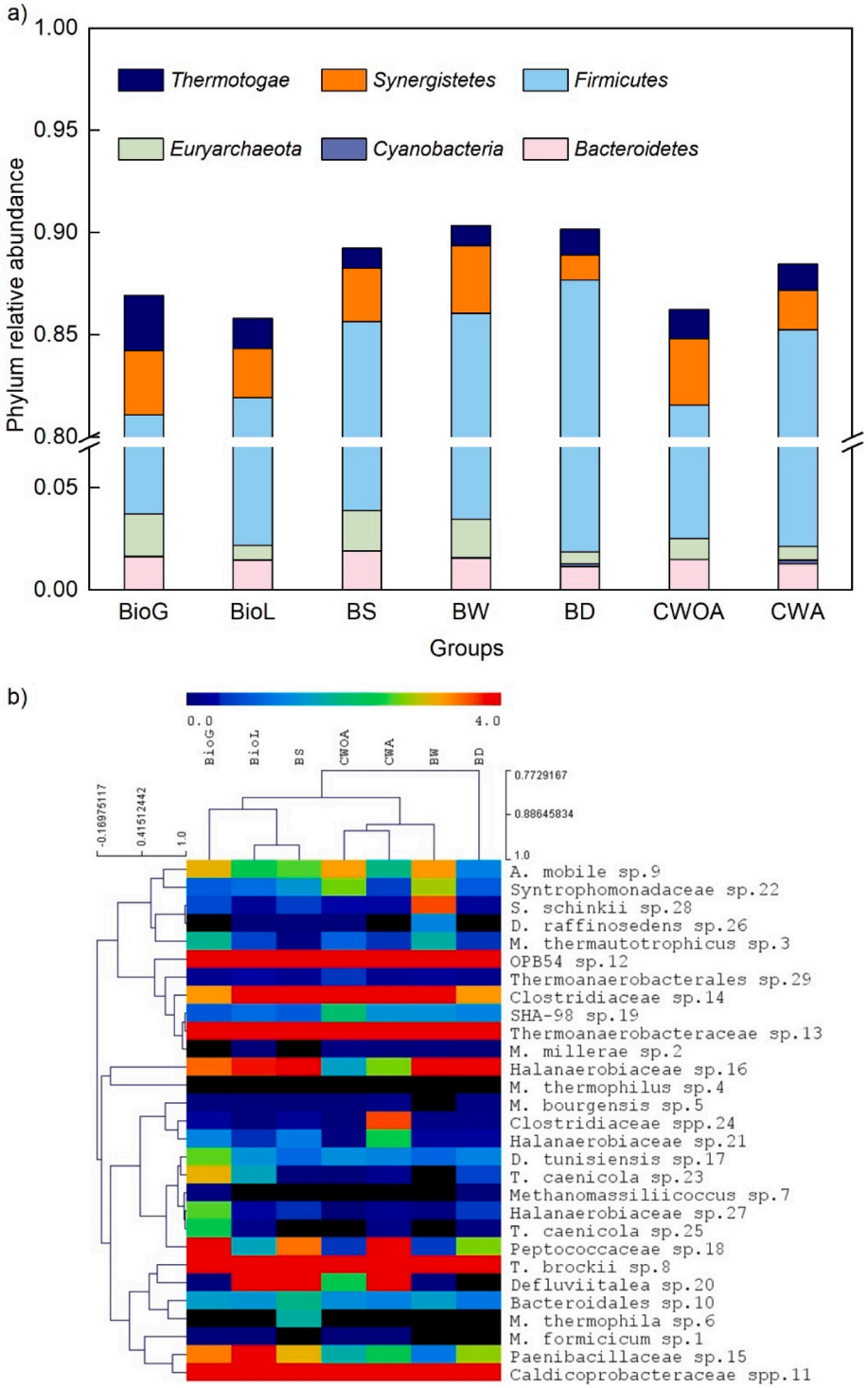

Fig. 4. a) Show the relative abundance of microbial composition (>1% at the phylum levels; and b) show the relative abundance of microbial composition (>1%) at the OTU level. BioG: Bioaugmentation using gel preserved consortium; BioL: Bioaugmentation using liquid fresh consortium; BS: Straw biochar; BW: Woodchip biochar; BD: Digestate biochar, CWOA: Control group without ammonia; CWA: Control group with ammonia.

precursors (Lackner et al., 2018). As *M. thermophila* sp.6 has a versatile methanogenic metabolism most frequently found as acetoclastic, thus we can assume this activity in BS. The archaeon growth seemed to be selectively stimulated by the unique characteristics of straw biochar or by this environment rich in acetate. Even though the relative abundance of *M. thermophila* sp.6 in BS was the same as *M. thermautotrophicus* sp.3 in BW, its effectiveness to alleviate ammonia stress was lower than *M. thermautotrophicus* sp.3, according to the values of R_{max}. These observations agreed with previous studies where hydrogenotrophic methanogens were found to contribute more to improving methane production of ammonia-stressed reactors than *Methanosarcina* (Capson-Tojo et al., 2020; Tian et al., 2019c). Many other works reported that *M. thermophila* excreted acetate into the surrounding medium during assimilation of CO_2 into cell carbon via intermediates (e.g., activated acetic acid or acetyl coenzyme A) (Lackner et al., 2018; Zhu et al., 2020). The re-uptake of lost acetate was limited by the minimum threshold (0.2

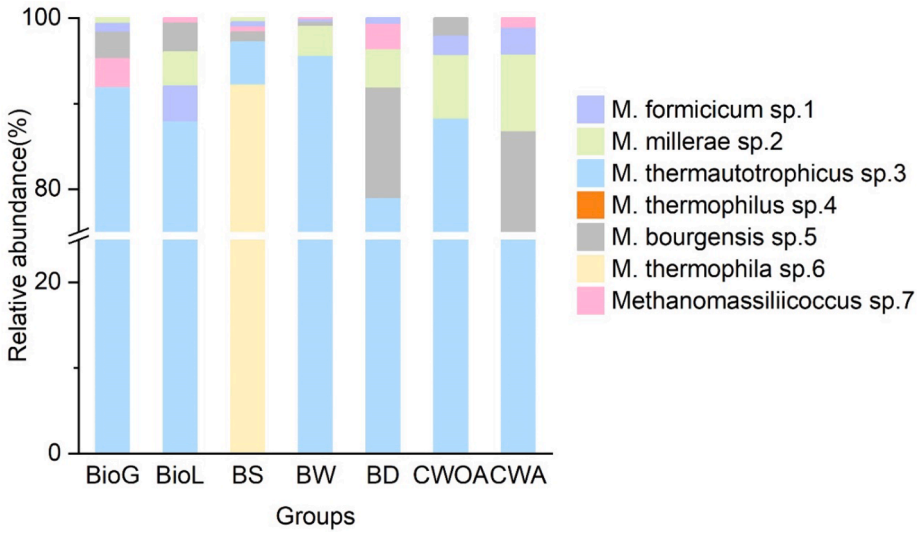

Fig. 5. Archaeal relative abundance (%) in different groups at species level.

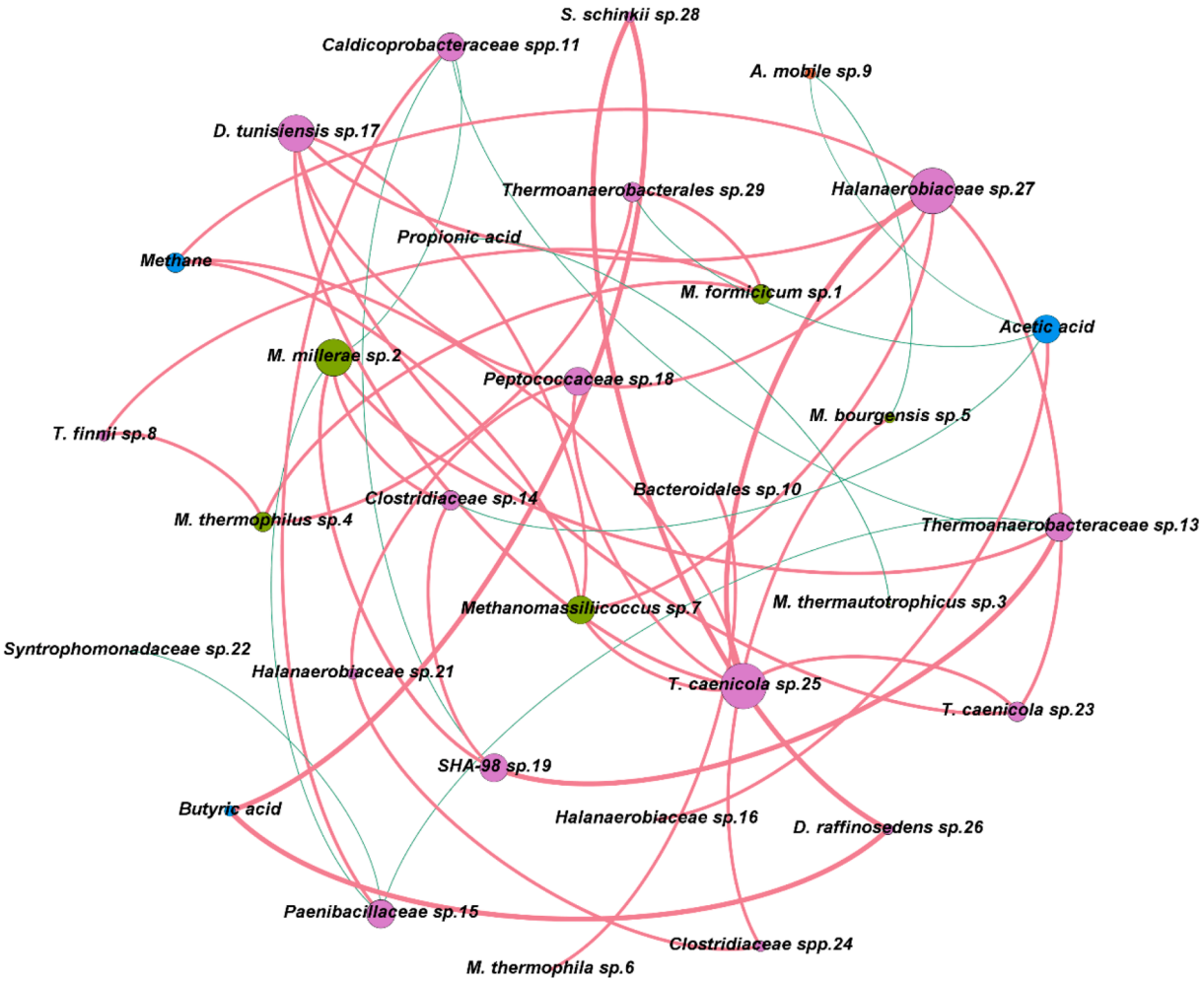

Fig. 6. Network analysis (spearman's correlation coefficient >0.6 and statistically significant (p-value) < 0.05) suggest potential cooperation (in red) or competition (in green) among relevant species with the key VFAs and methane yields. (For interpretation of the references to colour in this figure legend, the reader is referred to the web version of this article.)

to 1.2 mM) (Jetten et al., 1992). These metabolic features may explain the slow acetate degradation during the autotrophic methanogenesis by *M. thermophila* in the BS group dominated by the H_2/CO_2 producing bacteria.

4. Conclusions

This work for the first time demonstrated the potential of bioaugmentation with ready-to-use inocula to significantly accelerate ($p < 0.05$) the methane production rate and reduce the accumulation of acetate in ammonia-stressed anaerobic reactors. Woodchip biochar showed the excellent performance in ammonia remediation thanks to high surface area and electron conductivity capacity. Abundances of *M. thermautotrophicus* sp.3 was significantly enhanced with the application of gel preserved bioaugmentation inoculum and woodchip biochar, while *M. thermophila* sp.6 was selectively enriched in straw biochar. Thus, strategies of bioaugmentation using gel preserved consortium, woodchip biochar and straw biochar are recommended to recover ammonia-stressed anaerobic reactors.

Declaration of Competing Interest

The authors declare that they have no known competing financial interests or personal relationships that could have appeared to influence the work reported in this paper.

Acknowledgements

Miao Yan acknowledges the financial support from China Scholarship Council. Authors appreciate financial support from MUDP (Miljøstyrelsens) under the project framework FUBAF project (No. MST-117-00508) and VARGA project (No. MST-141-01377); and by EUDP (Energistyrelsen) under the project EFUEL (No. 64018-0559). Ioannis A. Fotidis acknowledges the financial support of National Natural Science Foundation of China, International Cooperation and Exchange Program "LyoCH$_4$-Development of novel lyophilized bioaugmentation inocula to alleviate ammonia toxicity in anaerobic reactors" (5185041512).

Appendix A. Supplementary data

Supplementary data to this article can be found online at https://doi.org/10.1016/j.biortech.2021.125329.

References

Ahn, J.-H., Do, T.H., Kim, S.D., Hwang, S., 2006. The effect of calcium on the anaerobic digestion treating swine wastewater. Biochem. Eng. J. 30 (1), 33–38.
Ambaye, T.G., Rene, E.R., Dupont, C., Wongrod, S., van Hullebusch, E.D., 2020. Anaerobic Digestion of Fruit Waste Mixed With Sewage Sludge Digestate Biochar: Influence on Biomethane Production. Front. Energy Res. 8, 14.
APHA, A. 2005. AWWA (2005) Standard methods for the examination of water and wastewater. American Public Health Association, Washington, DC.
Basaglia, M., Favaro, L., Torri, C., Casella, S., 2021. Is pyrolysis bio-oil prone to microbial conversion into added-value products? Renewable Energy 163, 783–791.
Bastian, M., Heymann, S., Jacomy, M. 2009. Gephi: an open source software for exploring and manipulating networks. Proceedings of the International AAAI Conference on Web and Social Media.
Campanaro, S., Treu, L., Kougias, P.G., Luo, G., Angelidaki, I., 2018. Metagenomic binning reveals the functional roles of core abundant microorganisms in twelve full-scale biogas plants. Water Res. 140, 123–134.
Campanaro, S., Treu, L., Rodriguez-R, L.M., Kovalovszki, A., Ziels, R.M., Maus, I., Zhu, X., Kougias, P.G., Basile, A., Luo, G., Schlüter, A., Konstantinidis, K.T., Angelidaki, I., 2020. New insights from the biogas microbiome by comprehensive genome-resolved metagenomics of nearly 1600 species originating from multiple anaerobic digesters. Biotechnol. Biofuels 13 (1). https://doi.org/10.1186/s13068-020-01679-y.
Cao, Y., Pawłowski, A., 2012. Sewage sludge-to-energy approaches based on anaerobic digestion and pyrolysis: Brief overview and energy efficiency assessment. Renew. Sustain. Energy Rev. 16 (3), 1657–1665.
Capson-Tojo, G., Moscoviz, R., Astals, S., Robles, Á., Steyer, J.-P., 2020. Unraveling the literature chaos around free ammonia inhibition in anaerobic digestion. Renew. Sustain. Energy Rev. 117, 109487.
Dyksma, S., Jansen, L., Gallert, C., 2020. Syntrophic acetate oxidation replaces acetoclastic methanogenesis during thermophilic digestion of biowaste. Microbiome 8 (1), 1–14.
Fotidis, I.A., Karakashev, D., Angelidaki, I., 2013. Bioaugmentation with an acetate-oxidising consortium as a tool to tackle ammonia inhibition of anaerobic digestion. Bioresour Technol 146, 57–62.
Frank, J., Arntzen, M.Ø., Sun, L., Hagen, L.H., McHardy, A., Horn, S.J., Eijsink, V.G., Schnürer, A., Pope, P.B., 2016. Novel syntrophic populations dominate an ammonia-tolerant methanogenic microbiome. Msystems 1 (5), e00092–e116.
Hansen, V., Müller-Stöver, D., Ahrenfeldt, J., Holm, J.K., Henriksen, U.B., Hauggaard-Nielsen, H., 2015. Gasification biochar as a valuable by-product for carbon sequestration and soil amendment. Biomass Bioenergy 72, 300–308.
Hu, X., Zhang, X., Ngo, H.H., Guo, W., Wen, H., Li, C., Zhang, Y., Ma, C., 2020. Comparison study on the ammonium adsorption of the biochars derived from different kinds of fruit peel. Sci. Total Environ. 707, 135544.
Jetten, M.S., Stams, A.J., Zehnder, A.J., 1992. Methanogenesis from acetate: a comparison of the acetate metabolism in Methanothrix soehngenii and Methanosarcina spp. FEMS Microbiol. Rev. 8 (3–4), 181–197.
Lackner, N., Hintersonnleitner, A., Wagner, A.O., Illmer, P., 2018. Hydrogenotrophic Methanogenesis and Autotrophic Growth of Methanosarcina thermophila. Archaea 2018, 4712608.
Lü, F., Liu, Y., Shao, L., He, P., 2019. Powdered biochar doubled microbial growth in anaerobic digestion of oil. Appl. Energy 247, 605–614.
Luo, G., De Francisci, D., Kougias, P.G., Laura, T., Zhu, X., Angelidaki, I., 2015. New steady-state microbial community compositions and process performances in biogas reactors induced by temperature disturbances. Biotechnol. Biofuels 8 (1), 1–10.
Masebinu, S., Akinlabi, E., Muzenda, E., Aboyade, A., 2019. A review of biochar properties and their roles in mitigating challenges with anaerobic digestion. Renew. Sustain. Energy Rev. 103, 291–307.
Mumme, J., Srocke, F., Heeg, K., Werner, M., 2014. Use of biochars in anaerobic digestion. Bioresour. Technol. 164, 189–197.
Qiu, L., Deng, Y., Wang, F., Davaritouchaee, M., Yao, Y., 2019. A review on biochar-mediated anaerobic digestion with enhanced methane recovery. Renew. Sustain. Energy Rev. 115, 109373.
Romero-Güiza, M., Mata-Alvarez, J., Chimenos, J., Astals, S., 2016. The effect of magnesium as activator and inhibitor of anaerobic digestion. Waste Manage. 56, 137–142.
Schmidt, H., Bucheli, T., Kammann, C., Glaser, B., Abiven, S., Leifeld, J. 2013. EBC (2012)'European Biochar Certificate-Guidelines for a Sustainable Production of Biochar. European Biochar Foundation (EBC).
Schober, P., Boer, C., Schwarte, L.A., 2018. Correlation Coefficients: Appropriate Use and Interpretation. Anesth. Analg. 126 (5), 1763–1768.
Sun, T., Levin, B.D., Schmidt, M.P., Guzman, J.J., Enders, A., Martínez, C.E., Muller, D. A., Angenent, L.T., Lehmann, J., 2018. Simultaneous quantification of electron transfer by carbon matrices and functional groups in pyrogenic carbon. Environ. Sci. Technol. 52 (15), 8538–8547.
Sun, Y., Yu, I.K.M., Tsang, D.C.W., Cao, X., Lin, D., Wang, L., Graham, N.J.D., Alessi, D.S., Komárek, M., Ok, Y.S., Feng, Y., Li, X.-D., 2019. Multifunctional iron-biochar composites for the removal of potentially toxic elements, inherent cations, and hetero-chloride from hydraulic fracturing wastewater. Environ. Int. 124, 521–532.
Tian, H., Fotidis, I.A., Kissas, K., Angelidaki, I., 2018. Effect of different ammonia sources on aceticlastic and hydrogenotrophic methanogens. Bioresour. Technol. 250, 390–397.
Tian, H., Mancini, E., Treu, L., Angelidaki, I., Fotidis, I.A., 2019a. Bioaugmentation strategy for overcoming ammonia inhibition during biomethanation of a protein-rich substrate. Chemosphere 231, 415–422.
Tian, H., Treu, L., Konstantopoulos, K., Fotidis, I.A., Angelidaki, I., 2019b. 16s rRNA gene sequencing and radioisotopic analysis reveal the composition of ammonia acclimatized methanogenic consortia. Bioresour. Technol. 272, 54–62.
Tian, H., Yan, M., Treu, L., Angelidaki, I., Fotidis, I.A., 2019c. Hydrogenotrophic methanogens are the key for a successful bioaugmentation to alleviate ammonia inhibition in thermophilic anaerobic digesters. Bioresour. Technol. 122070.
Tian, S.-Q., Wang, L., Liu, Y.-L., Ma, J., 2020. Degradation of organic pollutants by ferrate/biochar: Enhanced formation of strong intermediate oxidative iron species. Water Res. 183, 116054.
Treu, L., Kougias, P., de Diego-Díaz, B., Campanaro, S., Bassani, I., Fernández-Rodríguez, J., Angelidaki, I., 2018. Two-year microbial adaptation during hydrogen-mediated biogas upgrading process in a serial reactor configuration. Bioresour. Technol. 264, 140–147.
Treu, L., Tsapekos, P., Peprah, M., Campanaro, S., Giacomini, A., Corich, V., Kougias, P. G., Angelidaki, I., 2019. Microbial profiling during anaerobic digestion of cheese whey in reactors operated at different conditions. Bioresour. Technol. 275, 375–385.
Wan, Z., Sun, Y., Tsang, D.C., Hou, D., Cao, X., Zhang, S., Gao, B., Ok, Y.S., 2020. Sustainable remediation with an electroactive biochar system: mechanisms and perspectives. Green Chem. 22 (9), 2688–2711.
Wang, T., Zhang, D., Dai, L., Dong, B., Dai, X., 2018. Magnetite triggering enhanced direct interspecies electron transfer: a scavenger for the blockage of electron transfer in anaerobic digestion of high-solids sewage sludge. Environ. Sci. Technol. 52 (12), 7160–7169.
Wei, W., Guo, W., Ngo, H.H., Mannina, G., Wang, D., Chen, X., Liu, Y., Peng, L., Ni, B.-J., 2020. Enhanced high-quality biomethane production from anaerobic digestion of primary sludge by corn stover biochar. Bioresour. Technol. 123159.
Westerholm, M., Levén, L., Schnürer, A., 2012. Bioaugmentation of syntrophic acetate-oxidizing culture in biogas reactors exposed to increasing levels of ammonia. Appl. Environ. Microbiol. 78 (21), 7619–7625.

Xie, S., Yu, G., Ma, J., Wang, G., Wang, Q., You, F., Li, J., Wang, Y., Li, C., 2020. Chemical speciation and distribution of potentially toxic elements in soilless cultivation of cucumber with sewage sludge biochar addition. Environ. Res. 191, 110188.

Yan, M., Fotidis, I.A., Jéglot, A., Treu, L., Tian, H., Palomo, A., Zhu, X., Angelidaki, I., 2020a. Long-term preserved and rapidly revived methanogenic cultures: Microbial dynamics and preservation mechanisms. J. Cleaner Prod. 121577.

Yan, M., Fotidis, I.A., Jéglot, A., Treu, L., Tian, H., Palomo, A., Zhu, X., Angelidaki, I., 2020b. Long-term preserved and rapidly revived methanogenic cultures: Microbial dynamics and preservation mechanisms. J. Cleaner Prod. 263, 121577.

Yan, M., Fotidis, I.A., Tian, H., Khoshnevisan, B., Treu, L., Tsapekos, P., Angelidaki, I., 2019. Acclimatization contributes to stable anaerobic digestion of organic fraction of municipal solid waste under extreme ammonia levels: Focusing on microbial community dynamics. Bioresour. Technol. 286, 121376. https://doi.org/10.1016/j.biortech.2019.121376.

Yan, M., Treu, L., Campanaro, S., Tian, H., Zhu, X., Khoshnevisan, B., Tsapekos, P., Angelidaki, I., Fotidis, I.A., 2020c. Effect of ammonia on anaerobic digestion of municipal solid waste: inhibitory performance, bioaugmentation and microbiome functional reconstruction. Chem. Eng. J. 126159.

Yan, M., Treu, L., Zhu, X., Tian, H., Basile, A., Fotidis, I.A., Campanaro, S., Angelidaki, I., 2020d. Insights into ammonia adaptation and methanogenic precursor oxidation by genome-centric analysis. Environ. Sci. Technol. 54 (19), 12568–12582.

Yang, J., Zhao, Y., Ma, S., Zhu, B., Zhang, J., Zheng, C., 2016. Mercury removal by magnetic biochar derived from simultaneous activation and magnetization of sawdust. Environ. Sci. Technol. 50 (21), 12040–12047.

Zhang, M., Li, J., Wang, Y., Yang, C., 2019. Impacts of different biochar types on the anaerobic digestion of sewage sludge. RSC Adv. 9 (72), 42375–42386.

Zhao, Z., Zhang, Y., Woodard, T., Nevin, K., Lovley, D., 2015. Enhancing syntrophic metabolism in up-flow anaerobic sludge blanket reactors with conductive carbon materials. Bioresour. Technol. 191, 140–145.

Zhu, X., Campanaro, S., Treu, L., Seshadri, R., Ivanova, N., Kougias, P.G., Kyrpides, N., Angelidaki, I., 2020. Metabolic dependencies govern microbial syntrophies during methanogenesis in an anaerobic digestion ecosystem. Microbiome 8 (1), 22.